

Studies on the Chitin-Binding Property of Novel Cysteine-Rich Peptides from *Alternanthera sessilis*

*Shruthi G. Kini*¹, *Phuong Q. T. Nguyen*^{1,2}, *Sophie Weissbach*³, *Alvaro Mallagaray*³, *Joon Shin*¹, *Ho Sup Yoon*¹, *James P. Tam*^{1*}

¹School of Biological Sciences, Nanyang Technological University, Singapore - 637551

²Current address: Department of Chemistry, University of Rochester, Rochester, New York-14627-0216

³ Institut für Chemie, Universität zu Lübeck, Lübeck, Deutschland.

Abbreviations

GlcNAc – N-acetylglucosamine

AMP – Antimicrobial peptide

Ac-AMP – *Amaranthus caudatus*-AMP

CRP – Cysteine-rich peptide

aSG – altides G1-G3 from *Alternanthera sessilis* (green)

aSR – altides R1-R3 from *Alternanthera sessilis* (red)

D₂O - Deuterium oxide

EDTA- Ethylenediaminetetracetic acid

ER - Endoplasmic reticulum

HPLC - High-performance liquid chromatography

K_D – Dissociation constant

MALDI-TOF MS – Matrix-assisted laser desorption/ionization-time of flight mass spectrometry

NOESY - Nuclear overhauser effect spectroscopy

RACE - Rapid amplification of cDNA ends

RP – Reversed-phase

SCX – Strong cation exchange

COSY - Correlation spectroscopy

UPLC - Ultra-performance liquid chromatography

PCR – Polymerase chain reaction

Abstract

Hevein-like peptides are a family of cysteine-rich peptides (CRPs) and play a defensive role in plants against insects and fungal pathogens. In this study, we report the isolation and characterization of six hevein-like peptides, aSG1-G3 and aSR1-R3, collectively named altides from green and red varieties of *Alternanthera sessilis*, a perennial herb belonging to the Amaranthaceae family. Proteomic analysis of altides revealed they contain six cysteines (6C), seven glycines, four prolines, and a conserved chitin-binding domain (SXYGY/SXFGY). Thus far, only four 6C-hevein-like peptides have been isolated and characterized; hence, our study expands the existing library of these peptides. Nuclear magnetic resonance (NMR) study of altides showed its three disulfide bonds were arranged in a cystine knot motif. As a consequence of this disulfide arrangement, they are stable against thermal and enzymatic degradation. Gene cloning studies revealed altides contain a three-domain precursor with an endoplasmic reticulum signal peptide followed by a mature CRP domain and a short C-terminal tail. This indicates that the biosynthesis of altides is through the secretory pathway. ¹H-NMR titration experiments showed that the 29-30 amino-acid-long altides bind to chitin oligomers with dissociation constants in the micromolar range. Aromatic residues in the chitin-binding domain of altides were involved in the binding interaction. To our knowledge, aSR1 is the smallest hevein-like peptide with dissociation constant towards chitotriose comparable to hevein and other hevein-like peptides. Together, our study expands the existing library of 6C-hevein-like peptides and provides insights into their structure, biosynthesis, and interaction with chitin oligosaccharides.

Plants are constantly under attack by microorganisms and pests. Although their immune system is not as complex as animals, they have evolved a multilayered immune system to resist pathogens (1). In plants, the interaction between defense peptides and the chitin-containing cell wall of fungi and exoskeleton of insects is an important mechanism for fending off pathogenic attacks. Defense peptides that bind chitin, a polysaccharide-containing repeating β -(1-4)-linked N-acetylglucosamine (GlcNAc) units, are cysteine-rich peptides (CRPs) belonging to the hevein family. Archer *et al.* isolated hevein, the prototypic member of this family, from the latex of the rubber tree *Hevea brasiliensis* in 1960 (2). Hevein was found to have potent antifungal activity *in vitro* (2-4) and reportedly the major component in latex responsible for human latex-fruit allergy syndrome (4, 5). Since then, a number of hevein-like peptides, such as pseudohevein, *Urtica dioica* agglutinin, and *Amaranthus caudatus*-AMPs (Ac-AMPs) have been isolated (6-8). These 29-43-amino-acid peptides contain a chitin-binding motif (9), also called the hevein domain (10), consisting of conserved glycine, cysteine, and aromatic residues stabilized by three to five disulfide bonds.

Hevein-like peptides can be classified into three groups based on the number of cysteine residues, namely 6C-, 8C-, and 10C-hevein-like peptides. Among them, 6C-hevein-like peptides have attracted attention as they are the smallest hevein-like peptides capable of binding to chitin and eliciting antifungal activity. Examples of 6C-hevein-like peptides include Ac-AMP1 and Ac-AMP2, AMP isolated from *Amaranthus retroflexus* (Ar-AMP), and IWF-4 isolated from *Beta vulgaris*, all belonging to the Amaranthaceae family (11-13). These 6C-hevein-like peptides are 29-30 amino acids long and reported to have antifungal activity against a myriad of chitin-containing fungi (11, 12). Sequence comparison with hevein shows that 6C-hevein-like peptides contain a C-terminal deletion comprised of about 10 residues that includes the fourth disulfide bond. The three disulfide

bonds in 6C-hevein-like peptides exhibit a cystine knot arrangement (13) which confers improved stability against thermal and enzymatic degradation. Insight into the binding interactions of these minimum hevein domains with chitin may shed light on the molecular basis of their antifungal activity. The small size and high stability of 6C-hevein-like peptides make them interesting models for chitin binding studies.

In an effort to isolate more 6C-hevein-like peptides, we screened both red and green varieties of *Alternanthera sessilis*, a perennial herb belonging to the Amaranthaceae family (Fig. 1). Six novel CRPs, hereafter named altides G1-G3 or aSG1-G3 from *A. sessilis* (green) and altides R1-R3 or aSR1-R3 from *A. sessilis* (red), were isolated and characterized using proteomic and genomic methods. This study aims to provide insight into the sequence, structure, and binding interactions of altides with chitin oligosaccharides. Furthermore, our findings may facilitate the design of stable antifungal agents and/or development of transgenic crops with enhanced resistance to fungal infections.

Materials and Methods

General experimental procedures. High-performance liquid chromatography (HPLC) and ultra-performance liquid chromatography (UPLC) were performed on Shimadzu systems. Preparative, semi-preparative, and analytical reverse-phase (RP)-HPLC were performed on Phenomenex C18 columns (particle size, 5 μm ; pore size, 300 \AA ; Hesperia, CA, USA) with dimensions of 250 x 22 mm, 250 x 10 mm, and 250 x 4.6 mm, respectively. A polyLC polysulfoethyl A column (250 x 9.4 mm and 250 x 4.6 mm) was used for strong cation exchange (SCX)-HPLC. An ABI 4800 MALDI-TOF/TOF system (Applied Biosystems, Framingham, MA, USA) was used for mass spectrometry (MS) analysis of crude extracts and HPLC fractions. Absorbance in chitin binding, cytotoxicity, and hemolysis assays was acquired using an Infinite® 200 PRO microplate

reader (Tecan Group Ltd., Maennedorf, Switzerland Germany). Two-dimensional (2D)-NMR experiments were conducted with a Bruker Avance II 600 MHz NMR spectrometer (Bruker Instruments) equipped with a TXI-CryoProbe™, and ¹H-NMR titrations were performed with a Bruker Avance III 500 MHz NMR spectrometer equipped with a TCI-CryoProbe™ and a Bruker Avance II 400 MHz NMR spectrometer. All spectra were acquired at 298 K. Chemical reagents used in this study were of analytical grade and purchased from Sigma Aldrich (St. Louis, MO, USA).

Isolation of peptides from *A. sessilis*. *A. sessilis* (5-10 kg) was obtained from the Nanyang Technological University (Singapore) herb garden and minced in water. After removal of debris, the homogenized plant was extracted with water using a muslin cloth. The crude extract was centrifuged at 8000 rpm for 10 min at 4°C, and the clear supernatant was filtered and loaded on C₁₈ flash column. Elution was performed using increasing concentrations of ethanol (20-70%). Eluents that contained the desired peptides were pooled and purified using multiple rounds of SCX- and RP-HPLC. For SCX-HPLC, a linear gradient from buffer A (5% acetonitrile, 20 mM KH₂PO₄; pH 3) to buffer B (5% acetonitrile, 0.5 M KCl, 20 mM KH₂PO₄; pH 3) was used. Fractions from SCX-HPLC that contained chitin-binding peptides were pooled and purified by RP-HPLC using buffer A (0.1% trifluoroacetic acid in water) and buffer B (0.1% trifluoroacetic acid in 100% acetonitrile).

***De novo* sequencing of peptides using MALDI-TOF MS/MS.** Approximately 50 µg of peptide was incubated with 50 mM dithiothreitol at 60°C for 30 min to reduce disulfide bonds. Iodoacetamide (300 mM) was used to alkylate reduced disulfides. Trypsin,

chymotrypsin, and endo-GluC digestion was carried out for 5 min at room temperature, followed by MALDI-TOF MS/MS sequencing as described previously (14).

Chitin binding assay. Purified altides (20 μ M) were incubated with chitin beads (New England BioLabs, Singapore) in chitin binding buffer (140 mM NaCl, 10 mM Tris, 1 mM EDTA, 0.1% [v/v] Tween 20; pH 8.0) for 4 h. At each time point, the solution was centrifuged at 12,000 rpm for 1 min, and the absorbance of the supernatant was read at 280 nm. Elution of bound peptide was performed using two methods. In the first method, four chitin elution buffers (10 mM Tris, 1 mM EDTA, 0.1% [v/v] Tween 20; pH 8.0) with increasing NaCl concentration (300 mM, 500 mM, 700 mM, and 1 M) were used, and in the second method, 0.5 M acetic acid at 100°C for 30 min to 1 h was used. Supernatants were further analyzed using RP-UPLC and MALDI-TOF to assess binding and elution.

NMR spectroscopy. Samples containing approximately 0.5-0.6 mM peptide were prepared in a 20 mM sodium phosphate buffer (pH 7.0) containing 50 mM NaCl and 0.01% NaN₃ in D₂O or 10% D₂O. Nuclear Overhauser effect spectroscopy (NOESY) experiments were acquired with 200 and 300 ms mixing times (15, 16). Total correlation spectroscopy (COSY) (17) data were recorded with a mixing time of 69 or 78 ms using MLEV17 spin lock pulses (18). Vicinal coupling constants were measured using the double-quantum-filtered (DQF)-COSY (19) and one-dimensional (1D)-¹H-NMR experiments. All 2D-NMR data were recorded in the phase sensitive model using the time-proportional phase increment method (20), with 2048 data points in the t₂ domain and 512 points in the t₁ domain. Slowly-exchanging amide protons were identified by immediate acquisition of a series of 1D-experiments after dissolving the lyophilized

peptide in a D₂O solution. The water signal was suppressed using water-gated pulse sequences (21) or excitation sculpting (22) combined with pulsed-field gradients. All NMR data were processed using Bruker TOPSPIN 2.1 or NMRPipe (23) programs on a Linux workstation and analyzed using Sparky 3.12 software. DQF-COSY spectra were processed on 8192 x 1024 data matrices to obtain a maximum digital resolution for coupling constant measurements. Sodium 3-(trimethylsilyl)-1-propanesulfonate (DSS-d6) was used as internal reference.

Structure calculations. Solution structures of aSG1 were calculated by hybrid distance geometry and a simulated annealing protocol in torsion angle space with CNS 1.2 (24). The three disulfide bonds were restrained in accordance with the disulfide bonding patterns based on the observed H β -H β NOEs from NOESY spectra by generation of covalent disulfide linkages during the initial molecular topology file generation stage using a CNS script. A total of 597 distance and 18 torsion angle constraints were used for structure calculations. NOE distance restraints were classified strong (1.8-3.0 Å), medium (1.8-3.5 Å), weak (1.8-5.0 Å), or very weak (1.8-6.0 Å) based on intensities derived from NOESY spectra recorded in 10% D₂O or 100% D₂O. To validate the disulfide bond connectivities, structure calculations & refinements were performed for 15 different disulfide bond patterns. Molecular topology files for 15 different disulfide bond connectivities were generated using molecular topology file generating script of CNS. 200 structures were calculated by distance geometry regularization and simulated annealing protocol out of which the lowest 18-20 structures were selected for each disulfide bond combination and average total energies were compared. Corrections for pseudo-atom representations were used for non-stereospecifically assigned methylene, methyl group, and aromatic ring protons (20).. Backbone dihedral angle restraints were derived from $^3J_{HN\alpha}$ coupling constants in DQF-COSY or 1D-¹H-NMR spectra in a H₂O solution (25, 26). Backbone dihedral restraints were $-55^\circ \pm 45^\circ$ ($^3J_{HN\alpha} < 6$

Hz) and $-120^\circ \pm 50^\circ$ ($3J_{HN\alpha} > 8$ Hz). Hydrogen bond donors were identified from proton-deuterium exchange experiments, and hydrogen bond acceptors were determined in the preliminary structure calculation stage. The 200 starting structures were generated and refined using a hybrid distance geometry-simulated annealing protocol (27-29) in the CNS 1.2 program. Finally, 18 final structures were selected by their total energy values for display and structural analysis. MOLMOL (30) and PyMOL (31) programs were used for structure visualization and PROCHECK-NMR (32) were used for structure validation.

NMR titration experiments. The binding affinity of aSG1 and aSR1 towards N, N'-diacetyl chitobiose, N, N', N''-triacetyl chitotriose, and N, N', N'', N''', N''''-pentacetyl chitopentose was determined by monitoring chemical shifts in $^1\text{H-NMR}$ spectra from a series of titrations. Samples contained 0.6 mM peptide in 20 mM sodium phosphate buffer (pH 7.4) in D_2O , using 100 μM of DSS-d6 as internal reference. Increasing concentrations of chitobiose [0.036-50.8 mM], chitotriose [0.1-4.8 mM], and chitopentose [0.1-4.8 mM] were then titrated while keeping the peptide concentration constant. Differences in chemical shifts of characteristic protons were plotted against sugar concentrations and fitted using Origin 9.0 according to equation (1) (33):

$$\Delta\delta_{\text{obs}} = \Delta\delta_{\text{max}} \frac{([P]_t + [L]_t + K_D) - \{([P]_t + [L]_t + K_D)^2 - 4[P]_t[L]_t\}^{1/2}}{2[P]_t} \quad (1)$$

where $\Delta\delta_{\text{obs}}$ is the change in the observed shift from the free state, $\Delta\delta_{\text{max}}$ is the maximum shift change upon saturation, $[P]_t$ is the total concentration of the peptide, and $[L]_t$ is the total concentration of the sugar (33).

Heat stability assay. Purified altides were incubated for 1 h at 100°C in water and subsequently subjected to UPLC. DALK, a short peptide known to be thermostable, was

used as a positive control, and the linear peptide RLYRRGRLYRRNHV (RV-14) synthesized in the laboratory was used as a negative control. MALDI-TOF MS was used to monitor peaks collected by UPLC.

Proteolytic enzyme stability assay. Purified altides were incubated with or without trypsin and pepsin at a final peptide to enzyme ratio of 20:1 (mol/mol) at 37°C for 6 h. RV-14 was used as a control. At each time point, 50 µl of each sample was subjected to UPLC, and the mass of the peaks collected was determined by MALDI-TOF MS.

Cytotoxicity Assay. PrestoBlue Cell Viability reagent (Invitrogen, Carlsbad, CA, USA) was used to test the cytotoxicity of altides. Cells were seeded in a 96-well microtitre plate (5×10^4 cells/ml) and incubated with 1-100 µM altides for 24 h at 37 °C. After incubation, 10 µl PrestoBlue reagent was added to the wells and incubated at 37 °C for 1 h. Subsequently, fluorescence was measured according to the manufacturer's protocol. Wells without altides served as controls.

Cloning of altide genes. Total RNA was extracted from *A. sessilis* using Trizol® reagent (Life Technologies, Carlsbad, CA, USA). 3'- and 5'-cDNA libraries were synthesized from the RNA using a 3'-system for Rapid Amplification of cDNA Ends (RACE; Invitrogen) and SMARTer™ RACE cDNA Amplification kit (Clontech, Takara Biotechnology, Dalian, China), respectively. Degenerate primers targeting regions PQCNHG (5'-CCTGGTCArTGyAAyCAyGG-3') and QGYCGTG (5'-CAAGGTTATTGyGGnACnGG-3') were used in the 3'-RACE polymerase chain reaction (PCR). Products of desired size were cloned using pGEM-T Easy® vector (Promega, Madison, WI, USA) and sequenced. Specific primers were designed using the

3'-untranslated region to amplify the 5'-end of the construct in 5'-RACE PCR. To study the location of introns, genomic DNA of the plant was extracted using cetyltrimethyl ammonium bromide (CTAB) buffer (34), and specific primers designed to recognize altide untranslated regions were used in PCR. Precursor sequences were aligned using the ClustalW multiple alignment tool of BioEdit (35) software, and signal sequences were determined using SignalP server (36).

Antibacterial assay. Antibacterial activity of altides was assessed using a radial diffusion assay as described elsewhere (37). Gram-positive strains of *Staphylococcus aureus* and gram-negative *Escherichia coli* were used. CT-8, a potent antimicrobial CRP isolated in our laboratory from *Clitoria ternatea*, was used as the positive control.

Results

Isolation and sequencing of peptides from *A. sessilis*. Preliminary screening of red and green varieties of *A. sessilis* using MALDI-TOF revealed clusters of peptides between 3-4 kDa (Fig. 2). Therefore, a scale-up extraction (5-10 kg of *A. sessilis* leaves) of the putative CRPs was performed. The isolated peptides were fully reduced, alkylated, digested using trypsin, chymotrypsin, and endo-GluC, and then subjected to *de novo* sequencing using tandem MS. aSG1-G3 and aSR1-R3 were found to be 29-30 amino acids in length with a high content of cysteine (6 residues), glycine (7 residues), and proline (4 residues), accounting for nearly 60% of the peptide sequence (Table 1). Sequence comparison between altides of the green variety revealed greater than 89% homology, while altides from red variety were 85% identical to each other. Sequences from red and green varieties were 75-90% homologous to each other (38). BLAST analysis revealed they belong to a family of hevein-like proteins containing a single

chitin-binding domain. Sequence comparison revealed a 70-90% homology among altides and other hevein-like peptides from different plant families. Sequence alignment showed a conserved C-terminal tyrosine residue and a conserved chitin-binding domain (SXFGY/SXYGY) (Fig. 3A).

Solution structure of aSG1 determined by NMR. All spin-spin systems of aSG1 were identified, and ~98% of proton resonances were unambiguously assigned (Suppl. Fig. 1; Table S1). The three disulfide bonds (Cys I-Cys IV, Cys II-Cys V, and Cys III-Cys VI) were confirmed by characteristic $d\beta\beta(i,j)$ NOEs between cysteine pairs (Fig. 3B). The NMR ensemble was calculated using 15 disulfide bond patterns and structural energies between them were compared (Table S2). Based on the result of energetic analysis for different disulfide combinations, patterns Cys I-Cys IV/Cys II-Cys V/Cys III-Cys VI, Cys I-Cys V/Cys II-Cys IV/Cys III-Cys VI and Cys I-Cys II/Cys III-Cys VI/Cys IV-Cys V showed low total energy values (30 to 66 kcal/mol) compared with other disulfide bond patterns with energy values ranging from 200 to 760 kcal/mol. Disulfide pattern Cys I-Cys IV/Cys II-Cys V/Cys III-Cys VI had the lowest total energy value of 29.90 ± 0.87 kcal/mol indicating that this disulfide bond pattern of aSG1 is energetically more favorable than other possible disulfide bond combinations and is in agreement with $H\beta$ - $H\beta$ connectivities observed from NMR spectrum. The solution structure of aSG1 was determined based on a total of 597 NMR-derived distance restraints and 18 dihedral angle restraints. The ensemble of 18 low-energy structures is shown (Fig. 4A). Root-mean-square deviation values relative to the mean coordinate of 18 conformers for residues Gly-3 to Gly-30 were 0.28 Å for backbone atoms and 1.11 Å for all heavy atoms. Sequential $d\alpha N(i,i+1)$ NOE connectivity together with values of $3JHN\alpha$ and hydrogen bond patterns were determined by amide hydrogen exchange experiments.

aSG1 was shown to be shaped by a combination of at least two extended β -sheets and tight turn structures. In addition, several strong $dNN(i,i+1)$ and medium or weak $d\alpha N(i,i+3)$, $dNN(i,i+2)$, and $dNN(i,i+3)$ NOEs were also observed in the C-terminal region (Pro-26 to Gly-30), indicating an α -helix-like conformation for these regions. The aSG1 structure consisted of two antiparallel, small α -sheets ($\beta 1$:Cys15-Cys16 and $\beta 2$:Gly20-Gly24), one α -helix-like segment, and several tight turns and loops, and its molecular shape was well-defined by a number of medium- and long-range NOEs (Fig. 4B). PROCHECK analysis indicated that all residues were distributed in the allowed region of the Ramachandran map. Overall topology of aSG1 was that of a compact globular molecule and seemed to be stabilized by several strong hydrogen bonds and three disulfide bridges.

Chitin binding activity. To assess chitin binding activity of altides, aSG1, aSR1, and aSR2 were incubated with chitin beads at 4 °C for 4 h. At specified time intervals, the absorbance of the supernatant was measured at 280 nm to monitor free peptides. UPLC profiles indicated that altides bound to chitin within 1 h (Fig. 5). The use of chitin elution buffers comprised of up to 1 M NaCl showed no increase in absorbance, indicating that peptides bound strongly to the chitin beads. The use of 0.5 M acetic acid and incubation at 100 °C was effective for elution of aSG1 and aSR2 within 30 min and aSR1 in 1 h as indicated by absorbance values and UPLC profiles. Together the data suggest that altides bind strongly to chitin and can be eluted by heating under acidic conditions.

1H -NMR titration of altides and GlcNAc oligomers. To obtain the K_{DS} for the interaction between altides and GlcNAc oligomers, 1H -NMR titrations were performed. Increasing concentrations of chitobiose and chitotriose were titrated into 0.6 mM aSG1

and aSR1, respectively, and $^1\text{H-NMR}$ spectra were recorded at each titration point. Significant changes in the chemical shifts of a number of peaks validated the formation of a complex between altides and chitin oligosaccharides. When chitobiose was titrated into aSG1, the difference in chemical shifts of peaks in the region between 7.0-8.0 ppm indicated involvements of aromatic residues in binding (Fig. 6). Tyr-28, Tyr-19, Tyr-21, and Gln-18 were found to be involved in the binding of aSG1 to chitobiose. Titration of chitotriose into aSR1 also showed peak shifts between 7.0-8.0 and 1.2-1.4 ppm with line broadening, indicating similar residues were involved in binding chitotriose. Due to sequence homology between aSG1 and aSR1, observed chemical shift values of aSR1 were compared with the assigned spectra of aSG1 to elucidate the residues involved in the binding interactions. Arg-17, Phe-19, Tyr-21, and Tyr-27 of aSR1 were involved in the binding interaction with chitotriose. Extensive line broadening was observed when chitopentose was titrated into aSG1 which could be due to the formation of aggregates (39, 40). Therefore, only the interaction of aSG1 and aSR1 with chitobiose and chitotriose, respectively, were used for calculating K_D s. Chemical shift values were plotted against sugar concentration (Fig. 7) and fitted to equation (1). Interestingly, although the K_D for the interaction between aSG1 and chitobiose was 9.6 ± 0.107 mM, the K_D for aSR1 and chitotriose was found to be only 97 ± 17.8 μM .

Heat and proteolytic stability. To assess stability of altides to thermal and enzymatic degradation, peptides were incubated at 100 °C for 1 h or with trypsin and pepsin for 6 h. UPLC and MS data showed that altides remained stable in the heat stability test with 97% of aSR1 and 91% of aSR2 remaining intact after 1 h (Fig. 8). Likewise, altides treated with trypsin and pepsin were stable against enzymatic degradation, with greater than 75% of peptides remaining intact after a 6-h incubation (Fig. 8). The linear peptide (RV-14)

synthesized in our laboratory was used as a control for all experiments and was completely degraded within 1 h of trypsin and 4 h of pepsin treatment.

Biological activity of altides. The cytotoxicity, as well as antibacterial activity, of altides was assayed. In our experiments, none of the altides showed significant cytotoxic or antibacterial effects at concentrations up to 100 μ M.

Cloning of altide-encoding genes. The cDNA library obtained from RNA of *A. sessilis* (green) was subjected to 3'- and 5'-RACE PCR to attain full-length gene of aSG1.

Primers designed to recognize 3'- and 5'-UTRs of this gene amplified the DNA sequences of aSG1 and aSG2. The 81-amino-acid-long precursors (Fig. 9A) contained a 24-amino-acid endoplasmic reticulum (ER) signal peptide followed by a mature CRP domain and a 25-amino-acid C-terminal tail. The mature domains differed at three positions: Pro-26 in aSG1 was absent in aSG2, and Gln-28 and Ala-51 in aSG1 were replaced by Glu-28 and Arg-51 in aSG2, respectively. Both the signal peptides and C-terminal tail were highly conserved and differed by only one amino acid residue.

Sequence comparison of RACE and DNA PCR products showed that there were no introns in the gene coding for altides.

Discussion

In this study, six novel 6C-hevein-like peptides, collectively named altides, from both green and red varieties of *A. sessilis* (Amaranthaceae family) were isolated and characterized by proteomic, genomic, and biophysical methods. Currently, only four 6C-hevein-like peptides have been studied, namely, two Ac-AMPs, one Ar-AMP, and one IWF-4, all belonging to the Amaranthaceae family (11, 12, 41). Structural analysis of

altides using NMR showed that the three disulfide bonds between Cys I-Cys IV, Cys II-Cys V, and Cys III-Cys VI were arranged in a knotted structure typically characterized as a ring formed by two disulfide bonds and the connecting backbone through which the third disulfide bond penetrates. This stable, knotted conformation, called a cystine knot, contributes to the stability of altides to thermal and enzymatic degradation.

Bioprocessing of altides is through the secretory pathway.

Gene cloning studies have shown that altides are ribosomally synthesized peptides with a three-domain precursor comprising an ER signal domain followed by a mature domain and C-terminal tail (42). This gene organization differs from other CRPs which generally contain a pro-domain before the mature CRP-domain (14, 43, 44). The presence of an ER signal domain suggests that the bioprocessing of altides follows the secretory pathway (45). The ER signal sequence is cleaved by signal peptidase. The 30-residue mature domain is then cleaved from the 25-33-amino-acid C-terminal tail (Fig. 9B). BLAST analysis of altide precursor peptides showed that they are similar to other 6C-hevein-like peptides, like Ac-AMP2 (46), Ar-AMP (11), and IWF-4 (41), as well as 10C-hevein-like peptides Wamp-1, Wamp-2, and Wamp-3 from *Triticum kiharae* seeds (47). Altide precursors show highest sequence similarity with Ac-AMP2 (81%) and Ar-AMP (66%). Altide precursors are five residues longer than IWF-4, while their signal peptides showed no sequence similarity. Wamp precursors were 36 residues longer than altide precursors due to the longer mature domain (45 residues) and an additional 10 residues in the signal peptide and C-terminal tail (Fig. 9A). Together, the data suggests that the overall organization of the precursor peptides is conserved among 6C-, 8C-, and 10C-hevein-like peptides and only vary by domain length. Knowledge of altide precursor structures

provides insight into their biosynthesis and may be beneficial for development of transgenic crops.

Binding interaction between altides and GlcNAc oligomers.

The K_D and residues involved in the binding interaction between altides and chitin oligosaccharides were elucidated using $^1\text{H-NMR}$ titration experiments. Aromatic residues, Tyr-19, Tyr-21, and Tyr-28 from aSG1 (Fig.10) and Phe-18, Tyr-20, and Tyr-27 from aSR1, occupying the conserved chitin-binding domain (SXYGY or SXFGY), were involved in binding to the chitin oligosaccharides. Our results are similar to previous reports on complexes of hevein (48), pseudo-hevein (8), WGA (49), and Ac-AMP2 (50) where the aromatic residues at conserved positions stabilize the complex through CH- π stacking interactions and van der Waal's contacts.

The K_D for the interaction between aSG1 and chitobiose was 9.6 mM, whereas it was 97 μM for the interaction between aSR1 and chitotriose, showing two orders-of-magnitude difference. This difference can be attributed to the increase in number of binding sites when chitotriose was used (51). This observation is in agreement with previous studies on the interaction of hevein with chitin oligosaccharides where binding strength of the interaction increased by one order-of-magnitude per GlcNAc residue ($n = 1-3$) (51). The binding constant of aSR1 to chitotriose is comparable to Ac-AMP2 (6) and hevein (51). Together, this data provides insights into the binding motif and affinity of altides to chitin oligosaccharides which can be used to efficiently design putative antifungal agents with enhanced stability and affinity to chitin.

In summary, the discovery of altides has helped to expand the list of 6C-hevein-like peptides from four to ten and to gain knowledge of sequence diversity of the chitin-

binding motif. Due to the small size of altides, their interaction with chitin oligosaccharides was studied to gain insight into their binding affinity and active site. ¹H-NMR titration experiments of aSR1, the smallest 6C-hevein-like peptide isolated thus far, revealed that aromatic residues occupying the conserved chitin-binding domain were involved in binding, and the K_D of the interaction was comparable to hevein. As a consequence of their ability to bind to chitin oligosaccharides, altides are potential antifungal agents. 2D-NMR studies revealed that the disulfide bonds were arranged in a cystine knot motif, conferring high resistance to heat and enzymatic degradation. The high stability and low cytotoxicity of altides makes them attractive for studying their antifungal activity against phytopathogenic fungi. Knowledge regarding the cDNA and gene organization of altides can be utilized to develop transgenic crops with putative enhanced resistance to fungal infections.

ACKNOWLEDGEMENTS

We thank Prof. Dr. Thomas Peters from Institut für Chemie, Universität zu Lübeck, Lübeck, Deutschland for his guidance and permission to use the NMR facility for NMR titration experiments.

Funding Sources

This research was supported in part by the Competitive Research Grant from the National Research Foundation in Singapore (**NRF-CRP8-2011-05**) and the Singaporean-German Joint Research Project Grant (MIRAVIR) (**SGP-PROG-008**).

Supporting Information

Proton NMR chemical shift assignments for aSG1, NH/C α H finger print region of 2D-NOESY spectrum (mixing time 300ms) of aSG1 recorded in 90%H₂O/10%D₂O at 298K. Sequential connectivity of each amino acid residues were shown by solid lines. Comparison

of the total structural energies between different disulfide bond patterns. This material is available free of charge via the Internet at <http://pubs.acs.org>.

References

1. Slavokhotova, A. A., Naumann, T. A., Price, N. P. J., Rogozhin, E. A., Andreev, Y. A., Vassilevski, A. A., and Odintsova, T. I. (2014) Novel mode of action of plant defense peptides - hevein-like antimicrobial peptides from wheat inhibit fungal metalloproteases, *Febs Journal* 281, 4754-4764.
2. Archer, B. L. (1960) The Proteins of Hevea brasiliensis Latex Isolation and Characterization of Crystalline Hevein, *J. Biochem* 75, 236-240.
3. Jan Van Parijs, W. F. B., Irwin J. Goldstein, and Willy J. Peumans. (1991) Hevein an antifungal protein from rubber-tree, *Planta* 183, 258-264.
4. Sanchez-Monge, R., Blanco, C., Perales, A. D., Collada, C., Carrillo, T., Aragoncillo, C., and Salcedo, G. (2000) Class I chitinases, the panallergens responsible for the latex-fruit syndrome, are induced by ethylene treatment and inactivated by heating, *J Allergy Clin Immunol* 106, 190-195.
5. Blanco, C., Diaz-Perales, A., Collada, C., Sanchez-Monge, R., Carrillo, T., Aragoncillo, C., and Salcedo, G. (2000) Cross-reactions in the latex-fruit syndrome: A relevant role of chitinases but not of cross-reactive carbohydrate determinants, *J Allergy Clin Immunol* 105, S238-S238.
6. Jiménez-Barbero, J., Javier Cañada, F., Asensio, J. L., Aboitiz, N., Vidal, P., Canales, A., Groves, P., Gabius, H.-J., and Siebert, H.-C. (2006) Hevein Domains: An Attractive Model to Study Carbohydrate-Protein Interactions at Atomic Resolution, *Adv. Carbohydr. Chem. Biochem* 60, 303-354.
7. Peumans, W. J., and Van Damme, E. J. (1998) Plant lectins: specific tools for the identification, isolation, and characterization of O-linked glycans, *Crit Rev Biochem Mol Biol* 33, 209-258.
8. Asensio J. L., Siebert H.C., Lieth, Claus-Wilhelm Claus-Wilhelm von der, José Laynez, J., Bruix, M., U.M. Soedjanaamadja, Beintema J.J., Javier Canada, F., Hans-Joachim G., and Jimenez-Barbero, J. (2000) NMR Investigations of Protein-Carbohydrate Interactions: Studies on the Relevance of Trp/Tyr Variations in Lectin Binding Sites as Deduced from Titration Microcalorimetry and NMR Studies on Hevein Domains. Determination of the NMR Structure of the Complex Between Pseudohevein and N,N',N''-Triacetylchitotriose, *Proteins* 40, 218-236.
9. Wright, H. T., Sandrasegaram, G., and Wright, C. S. (1991) Evolution of a family of N-acetylglucosamine binding proteins containing the disulfide-rich domain of wheat germ agglutinin, *J Mol Evol* 33, 283-294.
- (9)10. Drenth, J., Low, B. W., Richardson, J. S., and Wright, C. S. (1980) The Toxin-Agglutinin Fold - a New Group of Small Protein Structures Organized around a 4-Disulfide Core, *J. Biol. Chem* 255, 2652-2655.
11. Lipkin, A., Anisimova, V., Nikonorova, A., Babakov, A., Krause, E., Bienert, M., Grishin, E., and Egorov, T. (2005) An antimicrobial peptide Ar-AMP from amaranth (*Amaranthus retroflexus* L.) seeds, *Phytochemistry* 66, 2426-2431.
12. Willem F. Broekaert, W. M., Franky R. G. Terras, Miguel F. C. De Belle, Paul Proost, Jozef Van Damme, L. D., Magda Claeys, Sarah B. Rees, Jozef Vanderleyden, and Cammue, B. P. A. (1992) Antimicrobial peptides from *Amaranthus caudatus* seeds with sequence homology to the cysteine glycine-rich domain of chitin-binding proteins, *Biochemistry* 31, 4308-4314.

13. Paul K. Pallaghy, Katherine J. Nielsen., David J. Craik., and Norton, R. S. (1994) A common structural motif incorporating a cystine knot and a triple-stranded β -sheet in toxic and inhibitory polypeptides, *Protein Sci* 3, 1833-1839.
14. Nguyen, G. K., Zhang, S., Nguyen, N. T., Nguyen, P. Q., Chiu, M. S., Hardjojo, A., and Tam, J. P. (2011) Discovery and characterization of novel cyclotides originated from chimeric precursors consisting of albumin-1 chain a and cyclotide domains in the Fabaceae family, *J Biol Chem* 286, 24275-24287.
15. Jeener, J., Meier, B. H., Bachmann, P., and Ernst, R. R. (1979) Investigation of Exchange Processes by 2-Dimensional Nmr-Spectroscopy, *J Chem Phys* 71, 4546-4553.
16. Kumar, A., Ernst, R. R., and Wuthrich, K. (1980) A Two-Dimensional Nuclear Overhauser Enhancement (2d Noe) Experiment for the Elucidation of Complete Proton-Proton Cross-Relaxation Networks in Biological Macromolecules, *Biochem Biophys Res Commun* 95, 1-6.
17. Davis, D. G., and Bax, A. (1985) Assignment of Complex H-1-Nmr Spectra Via Two-Dimensional Homonuclear Hartmann-Hahn Spectroscopy, *J Am Chem Soc* 107, 2820-2821.
18. Bax, A. (1985) MLEV-17-based two-dimensional homonuclear magnetization transfer spectroscopy, *J. Magn. Reson* 65, 355-360.
19. Rance, M., Sorensen, O. W., Bodenhausen, G., Wagner, G., Ernst, R. R., and Wuthrich, K. (1983) Improved spectral resolution in cosy ^1H NMR spectra of proteins via double quantum filtering, *Biochem Biophys Res Commun* 117, 479-485.
20. Wuthrich, K., Billeter, M., and Braun, W. (1983) Pseudo-Structures for the 20 Common Amino-Acids for Use in Studies of Protein Conformations by Measurements of Intramolecular Proton Proton Distance Constraints with Nuclear Magnetic-Resonance, *J Mol Biol* 169, 949-961.
21. Liu, M., Mao, X.-A., Ye, C., Huang, H., Nicholson, J., and Lindon, J. (1998) Improved WATERGATE Pulse Sequences for Solvent Suppression in NMR Spectroscopy, *J Magn Reson* 132, 125-129.
22. Hwang, T. L., and Shaka, A. J. (1995) Water Suppression That Works. Excitation Sculpting Using Arbitrary Wave-Forms and Pulsed-Field Gradients, *J. Magn. Reson, Ser A* 112, 275-279.
23. Delaglio, F., Grzesiek, S., Vuister, G., Zhu, G., Pfeifer, J., and Bax, A. (1995) NMRPipe: A multidimensional spectral processing system based on UNIX pipes, *J Biomol Nmr* 6, 277-293.
24. Brunger, A. T., Adams, P. D., Clore, G. M., DeLano, W. L., Gros, P., Grosse-Kunstleve, R. W., Jiang, J. S., Kuszewski, J., Nilges, M., Pannu, N. S., Read, R. J., Rice, L. M., Simonson, T., and Warren, G. L. (1998) Crystallography & NMR system: A new software suite for macromolecular structure determination, *Acta Crystallogr D Biol Crystallogr* 54, 905-921.
25. Pardi, A., Billeter, M., and Wüthrich, K. (1984) Calibration of the angular dependence of the amide proton- Ca proton coupling constants, $3\text{JHN}\alpha$, in a globular protein, *J Mol Biol* 180, 741-751.
26. Driscoll, P. C., Gronenborn, A. M., Beress, L., and Clore, G. M. (1989) Determination of the three-dimensional solution structure of the antihypertensive and antiviral protein BDS-I from the sea anemone *Anemonia sulcata*: a study using nuclear magnetic resonance and hybrid distance geometry-dynamical simulated annealing, *Biochemistry* 28, 2188-2198.
27. Nilges, M., Clore, G. M., and Gronenborn, A. M. (1988) Determination of three-dimensional structures of proteins from interproton distance data by hybrid distance geometry-dynamical simulated annealing calculations, *FEBS Lett* 229, 317-324.
28. Nilges, M., Gronenborn, A., Brünger, A., and Clore, M. (1988) Determination of three-dimensional structures of proteins by simulated annealing with interproton distance restraints. Application to crambin, potato carboxypeptidase inhibitor and barley serine proteinase inhibitor 2, *Protein Eng* 2, 27-38.

29. Nilges, M. (1993) A calculation strategy for the structure determination of symmetric dimers by ¹H NMR, *Proteins* 17, 297-309.
30. Koradi, R., Billeter, M., and Wüthrich, K. (1996) MOLMOL: A program for display and analysis of macromolecular structures, *J. Mol. Graphics* 14, 51-55.
31. The PyMOL Molecular Graphics System, Version 1.7.4 Schrödinger, LLC.
32. Laskowski, R. A., MacArthur, M. W., Moss, D. S., and Thornton, J. M. (1993) PROCHECK: a program to check the stereochemical quality of protein structures, *J. Appl. Crystallogr* 26, 283-291.
33. Williamson, M. P. (2013) Using chemical shift perturbation to characterise ligand binding, *Prog. Nucl. Magn. Reson. Spectrosc.* 73, 1-16.
34. Doyle, J. J., and Doyle, J. L. (1987) A rapid DNA isolation procedure for small quantities of fresh leaf tissue, *Phytochem Bull.* 19, 11-15.
35. Petersen, T. N., Brunak, S., von Heijne, G., and Nielsen, H. (2011) SignalP 4.0: discriminating signal peptides from transmembrane regions, *Nature methods* 8, 785-786.
36. Hall, T. A. (1999) BioEdit: a user-friendly biological sequence alignment editor and analysis program for Windows 95/98/NT, *Nucleic Acids Symp Ser* 41, 95-98.
37. Lehrer, R. I., Rosenman, M., Harwig, S. S. S. L., Jackson, R., and Eisenhauer, P. (1991) Ultrasensitive Assays for Endogenous Antimicrobial Polypeptides, *J Immunol Methods* 137, 167-173.
38. Miller, X. H. a. W. (1991) A Time-Efficient, Linear-Space Local Similarity Algorithm *Adv Appl Math* 12 337-357.
39. Feeney, J., Batchelor, J. G., Albrand, J. P., and Roberts, G. C. K. (1979) Effects of Intermediate Exchange Processes on the Estimation of Equilibrium-Constants by Nmr, *J Magn Reson* 33, 519-529.
40. Lian, L. Y. (1993) Dynamic and exchange processes in macromolecules studied by NMR spectroscopy., *Method mol biol* 17, 169-189.
41. Klaus K. Nielsen, j. E. N., Susan M. Madrid, and Jorn D. Mikkelsen. (1997) Characterization of a New Antifungal Chitin-Binding Peptide from Sugar Beet Leaves, *Plant Physiol*, 83-91.
42. Jennings, C., West, J., Waive, C., Craik, D., and Anderson, M. (2001) Biosynthesis and insecticidal properties of plant cyclotides: The cyclic knotted proteins from *Oldenlandia affinis*, *P Natl Acad Sci USA* 98, 10614-10619.
43. Nguyen, G. K. T., Zhang, S., Wang, W., Wong, C. T. T., Nguyen, N. T. K., and Tam, J. P. (2011) Discovery of a Linear Cyclotide from the Bracelet Subfamily and Its Disulfide Mapping by Top-down Mass Spectrometry, *J Biol Chem* 286, 44833-44844.
44. Nguyen, P. Q. T., Luu, T. T., Bai, Y., Nguyen, G. K. T., Pervushin, K., and Tam, J. P. (2015) Allotides: Proline-Rich Cystine Knot α -Amylase Inhibitors from *Allamanda cathartica*, *Journal of Natural Products* 78, 695-704.
45. Mergaert, P., Nikovics, K., Kelemen, Z., Maunoury, N., Vaubert, D., Kondorosi, A., and Kondorosi, E. (2003) A novel family in *Medicago truncatula* consisting of more than 300 nodule-specific genes coding for small, secreted polypeptides with conserved cysteine motifs, *Plant Physiol* 132, 161-173.
46. De Bolle, M. F. C., David, K. M. M., Rees, S. B., Vanderleyden, J., Cammue, B. P., and Broekaert, W. F. (1993) Cloning and characterization of a cDNA encoding an antimicrobial chitin-binding protein from amaranth, *Amaranthus caudatus*, *Plant Mol Biol* 22, 1187-1190.
47. Andreev, Y. A., Korostyleva, T. V., Slavokhotova, A. A., Rogozhin, E. A., Utkina, L. L., Vassilevski, A. A., Grishin, E. V., Egorov, T. A., and Odintsova, T. I. (2012) Genes encoding hevein-like defense peptides in wheat: distribution, evolution, and role in stress response, *Biochimie* 94, 1009-1016.
48. Asensio, J. L., Canada, F. J., Bruix, M., Rodriguezromero, A., and Jimenezbarbero, J. (1995) The Interaction of Hevein with N-Acetylglucosamine-Containing Oligosaccharides - Solution Structure of Hevein Complexed to Chitobiose, *Eur J Biochem* 230, 621-633.

49. Juan Felix Espinosa, J. L. A., Jose Luis Garcia, Jose Laynez, Marta Bruix, Christine Wright, and Hans-Christian Siebert, H.-J. G., Francisco Javier Canada and Jesus Jimenez-Barbero. (2000) NMR investigations of protein-carbohydrate interactions binding studies and refined three-dimensional solution structure of the complex between the B domain of wheat germ agglutinin and N,N',N''-triacetylchitotriose, *Eur. J. Biochem* 267, 3965-3978.
50. Verheyden, P., Pletinckx, J., Maes, D., Pepermans, H. A. M., and Wyns, L. (1995) ¹H NMR study of the interaction of triacetyl chitotriose with Ac-AMP2, a sugar binding antimicrobial protein isolated from *A. caudatus*, *FEBS Lett* 370, 245-249.
51. Juan L Asensio, Cañada, Francisco J., Hans-Christian Siebert, José Laynez, Ana Poveda, Nieto, Pedro M., UM Soedjanaamadja, Hans-Joachim Gabius, and Jiménez-Barbero. (2000) Structural basis for chitin recognition by defense proteins: GlcNAc residues are bound in a multivalent fashion by extended binding sites in hevein domains , *Chem & Biol* 7, 529–543.

Tables

Peptide	Peptide Sequence	Molecular Weight (Da)	Charge
aSG1	APGQCNHGRCPSGLCCSQYGYCGTGPAYCG-	3004	+2
aSG2	A-GECNHGRCPSGLCCSQYGYCGTGPARYCG-	2992	+2
aSG3	APGQCNHGRCPSGICCSQYGYCGTGPAYCGG	3060	+2
aSR1	VGECVQGRCPPGLCCSRFGYCGTGPAYCG-	2932	+1
aSR2	APGECKHGRCPPGICCSQYGYCGTGPAYCG-	3029	+2
aSR3	APGECKHGRCPPGICCSQYGYCGTGPAYC--	2973	+2

Table 1. Primary sequence of altides isolated from red and green varieties of *A.sessilis*. Purified and isolated peptides were reduced, alkylated, digested and sequenced using tandem MS *de novo* sequencing

Figure Legends

Figure 1. (A) Aerial parts the green variety of *A.sessilis*. (B) Aerial parts of the red variety of *A.sessilis*

Figure 2. MALDI-TOF MS profile of aerial parts of (A) green variety and (B) red variety of *A.sessilis*. Fresh plant material (250 mg) was ground to fine pieces in 50% ethanol and the extract was analyzed by MALDI-TOF MS to check for presence of CRPs

Figure 3. Consensus sequences and secondary structure of altides of altides. (A) Altide sequences are aligned with sequences of 6C-, 8C- and 10C-hevein like peptides from different plants. All peptides show a conserved chitin-binding motif SXYGY/SXFGY/SXWGY. β stands for β -strand and α stands for α -helix. Disulfide connectivity is indicated by blue bridges. (B) Two-dimensional NOESY spectra showing the expanded aliphatic regions of aSG1 obtained with mixing time 300ms in D₂O at 25°C. The correlations between cysteines forming disulfide bridges of ASG1 (Cys⁵-H ^{β} /Cys¹⁶-H ^{β} , Cys¹⁰-H ^{β} /Cys²²-H ^{β} , Cys¹⁵-H ^{β} /Cys²⁹-H ^{β}) are represented by rectangular boxes.

Figure 4. NMR structure of aSG1. A) Superposition of the backbone traces from final 18 ensembles of solution structures and restrained energy minimized (REM) structure of aSG1 by NMR spectroscopy. REM structure of aSG1 was highlighted in red color. B) Ribbon representation of aSG1 REM structure. Three disulfide bridges (Cys I-Cys IV, Cys II-Cys V and Cys III-Cys VI) are shown by ball and stick representation.

Figure 5. Chitin binding activity of altides. After incubation with chitin beads for 4 h at 4°C, UPLC profiles showed that aSG1 (A), aSR1 (B), aSR2 (C) bound to the beads in 1 h. Bound altides were eluted in acidic condition with heating at 100°C. aSG1 (D) and aSR2 (F) were eluted in 30 min while aSR1 (E) was eluted in 1 h

Figure 6. ¹H-NMR titration study of altides with chitin oligosaccharides. **(A)** 0.6 mM aSG1 was titrated with increasing concentration of chitobiose at pH 7.4. Variations in protons of tyrosine residues were followed. Sugar concentration is indicated on the left. **(B)** Increasing concentration of chitotriose was titrated into 0.6 mM aSR1. Dramatic changes in chemical shift and line broadening of peaks corresponding to aromatic residues were observed. chitotriose concentration is indicated on the left

Figure 7. ¹H NMR titration plots for **(A)** aSG1 and chitobiose and **(B)** aSR1 and chitotriose with corresponding dissociation constants. **(C)** ¹H NMR spectrum of aSR1 with the assigned ¹H NMR spectrum of aSG1 indicating the residues involved in the binding interaction

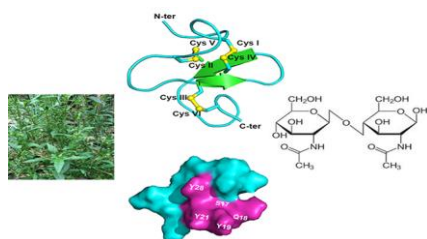
Figure 8. Stability assays of altides. Thermal stability of aSR1 **(A)** and aSR2 **(B)** at 100°C. DALK, a linear peptide synthesized in our laboratory was used as an internal standard. **(C)** Trypsin stability of aSR1. **(D)** Pepsin stability assay of aSR1. aSR1 remained stable to thermal and enzymatic degradation

Figure 9. Precursor structure of altides. **(A)** Alignment of altide precursors with precursors of other hevein-like peptides including Ac-AMP2, Ar-AMP, IWF-4, WAMP-1, WAMP-2 and WAMP-3. **(B)** Biosynthesis pathway of altides

Figure 10. Chitin-binding motif of aSG1. ¹H-NMR titrations with chitobiose showed that Gln-18, Tyr-19, Tyr-21 and Tyr-28 were involved in binding interaction.

Studies on the Chitin-Binding Property of Novel Cysteine-Rich Peptides from *Alternanthera sessilis*

Shruthi G. Kini¹, Phuong Q. T. Nguyen^{1,2}, Sophie Weissbach³, Alvaro Mallagaray³, Joon Shin¹, Ho Sup Yoon¹, James P. Tam¹*



1. Slavokhotova, A. A., Naumann, T. A., Price, N. P. J., Rogozhin, E. A., Andreev, Y. A., Vassilevski, A. A., and Odintsova, T. I. (2014) Novel mode of action of plant defense peptides - hevein-like antimicrobial peptides from wheat inhibit fungal metalloproteases, *Febs Journal* 281, 4754-4764.
2. Archer, B. L. (1960) The Proteins of Hevea brasiliensis Latex Isolation and Characterization of Crystalline Hevein, *Journal of Biochemistry*, 236-240.
3. Jan Van Parijs 1, W. F. B., Irwin J. Goldstein 2, and Willy J. Peumans 1. (1990) Hevein an antifungal protein from rubber-tree, *Planta* 258-264.
4. Sanchez-Monge, R., Blanco, C., Perales, A. D., Collada, C., Carrillo, T., Aragoncillo, C., and Salcedo, G. (2000) Class I chitinases, the panallergens responsible for the latex-fruit syndrome, are induced by ethylene treatment and inactivated by heating, *J Allergy Clin Immunol* 106, 190-195.
5. Blanco, C., Diaz-Perales, A., Collada, C., Sanchez-Monge, R., Carrillo, T., Aragoncillo, C., and Salcedo, G. (2000) Cross-reactions in the latex-fruit syndrome: A relevant role of chitinases but not of cross-reactive carbohydrate determinants, *J Allergy Clin Immunol* 105, S238-S238.
6. Jiménez-Barbero, J., Javier Cañada, F., Asensio, J. L., Aboitiz, N., Vidal, P., Canales, A., Groves, P., Gabius, H.-J., and Siebert, H.-C. (2006) Hevein Domains: An Attractive Model to Study Carbohydrate-Protein Interactions at Atomic Resolution, *Advances in carbohydrate chemistry and biochemistry* 60, 303-354.

7. Peumans, W. J., and Van Damme, E. J. (1998) Plant lectins: specific tools for the identification, isolation, and characterization of O-linked glycans, *Crit Rev Biochem Mol Biol* 33, 209-258.
8. Juan Luis Asensio, H.-C. S., Claus-Wilhelm von der Lieth, Jose´ Laynez, Marta Bruix,, U.M. Soedjanaamadja, J. J. B., Francisco Javier Canada, Hans-Joachim Gabius, and, and Jimenez-Barbero*, J. (2000) <NMR Investigations of Protein-Carbohydrate Interactions:Studies on the Relevance of Trp/Tyr Variations in Lectin Binding Sites as Deduced from Titration Microcalorimetry and NMR Studies on Hevein Domains. Determination of the NMR Structure of the Complex Between Pseudohevein and N,N',N''-Triacetylchitotriose.pdf>, *Proteins: Structure, Function, and Genetics*, 218–236.
9. Wright, H. T., Sandrasegaram, G., and Wright, C. S. (1991) Evolution of a family of N-acetylglucosamine binding proteins containing the disulfide-rich domain of wheat germ agglutinin, *J Mol Evol* 33, 283-294.
10. Drenth, J., Low, B. W., Richardson, J. S., and Wright, C. S. (1980) The Toxin-Agglutinin Fold - a New Group of Small Protein Structures Organized around a 4-Disulfide Core, *Journal of Biological Chemistry* 255, 2652-2655.
11. Lipkin, A., Anisimova, V., Nikonorova, A., Babakov, A., Krause, E., Bienert, M., Grishin, E., and Egorov, T. (2005) An antimicrobial peptide Ar-AMP from amaranth (*Amaranthus retroflexus* L.) seeds, *Phytochemistry* 66, 2426-2431.
12. Willem F. Broekaert, W. M., Franky R. G. Terras, Miguel F. C. De Belle, Paul Proost,, Jozef Van Damme, L. D., Magda Claeys, Sarah B. Rees, Jozef Vanderleyden, and, and Cammue, B. P. A. (1992) Antimicrobial peptides from *Amaranthus caudatus* seeds with sequence homology to the cysteine glycine-rich domain of chitin-binding proteins, *Biochemistry* 31, 4308-4314.
13. Paul K. Pallaghy, K. J. N., David J. Craik,, and Norton, R. S. (1994) <A common structural motif incorporating a cystine knot and a triple-stranded B-sheet in toxic and inhibitory polypeptides.pdf>, *Protein Science*, 1833-1839.
14. Nguyen, G. K., Zhang, S., Nguyen, N. T., Nguyen, P. Q., Chiu, M. S., Hardjojo, A., and Tam, J. P. (2011) Discovery and characterization of novel cyclotides originated from chimeric precursors consisting of albumin-1 chain a and cyclotide domains in the Fabaceae family, *J Biol Chem* 286, 24275-24287.
15. Jeener, J., Meier, B. H., Bachmann, P., and Ernst, R. R. (1979) Investigation of Exchange Processes by 2-Dimensional Nmr-Spectroscopy, *J Chem Phys* 71, 4546-4553.
16. Kumar, A., Ernst, R. R., and Wuthrich, K. (1980) A Two-Dimensional Nuclear Overhauser Enhancement (2d Noe) Experiment for the Elucidation of Complete Proton-Proton Cross-Relaxation Networks in Biological Macromolecules, *Biochem Biophys Res Commun* 95, 1-6.
17. Davis, D. G., and Bax, A. (1985) Assignment of Complex H-1-Nmr Spectra Via Two-Dimensional Homonuclear Hartmann-Hahn Spectroscopy, *J Am Chem Soc* 107, 2820-2821.
18. Bax, A. (1985) MLEV-17-based two-dimensional homonuclear magnetization transfer spectroscopy, *Journal of Magnetic Resonance (1969)* 65, 355-360.
19. Rance, M., Sorensen, O. W., Bodenhausen, G., Wagner, G., Ernst, R. R., and Wuthrich, K. (1983) Improved spectral resolution in cosy 1H NMR spectra of proteins via double quantum filtering, *Biochem Biophys Res Commun* 117, 479-485.
20. Wuthrich, K., Billeter, M., and Braun, W. (1983) Pseudo-Structures for the 20 Common Amino-Acids for Use in Studies of Protein Conformations by Measurements of Intramolecular Proton Proton Distance Constraints with Nuclear Magnetic-Resonance, *J Mol Biol* 169, 949-961.
21. Liu, M., Mao, X.-A., Ye, C., Huang, H., Nicholson, J., and Lindon, J. (1998) Improved WATERGATE Pulse Sequences for Solvent Suppression in NMR Spectroscopy, *J Magn Reson* 132, 125-129.
22. Hwang, T. L., and Shaka, A. J. (1995) Water Suppression That Works. Excitation Sculpting Using Arbitrary Wave-Forms and Pulsed-Field Gradients, *Journal of Magnetic Resonance, Series A* 112, 275-279.
23. Delaglio, F., Grzesiek, S., Vuister, G., Zhu, G., Pfeifer, J., and Bax, A. (1995) NMRPipe: A multidimensional spectral processing system based on UNIX pipes, *J Biomol Nmr* 6, 277-293.

24. Brunger, A. T., Adams, P. D., Clore, G. M., DeLano, W. L., Gros, P., Grosse-Kunstleve, R. W., Jiang, J. S., Kuszewski, J., Nilges, M., Pannu, N. S., Read, R. J., Rice, L. M., Simonson, T., and Warren, G. L. (1998) Crystallography & NMR system: A new software suite for macromolecular structure determination, *Acta Crystallogr D Biol Crystallogr* 54, 905-921.
25. Pardi, A., Billeter, M., and Wüthrich, K. (1984) Calibration of the angular dependence of the amide proton-C α proton coupling constants, $^3J_{HN\alpha}$, in a globular protein, *J Mol Biol* 180, 741-751.
26. Driscoll, P. C., Gronenborn, A. M., Beress, L., and Clore, G. M. (1989) Determination of the three-dimensional solution structure of the antihypertensive and antiviral protein BDS-I from the sea anemone *Anemonia sulcata*: a study using nuclear magnetic resonance and hybrid distance geometry-dynamical simulated annealing, *Biochemistry* 28, 2188-2198.
27. Nilges, M., Clore, G. M., and Gronenborn, A. M. (1988) Determination of three-dimensional structures of proteins from interproton distance data by hybrid distance geometry-dynamical simulated annealing calculations, *FEBS Lett* 229, 317-324.
28. Nilges, M., Gronenborn, A., Brünger, A., and Clore, M. (1988) Determination of three-dimensional structures of proteins by simulated annealing with interproton distance restraints. Application to crambin, potato carboxypeptidase inhibitor and barley serine proteinase inhibitor 2, *Protein Eng* 2, 27-38.
29. Nilges, M. (1993) A calculation strategy for the structure determination of symmetric dimers by 1H NMR, *Proteins: Structure, Function, and Bioinformatics* 17, 297-309.
30. Koradi, R., Billeter, M., and Wüthrich, K. (1996) MOLMOL: A program for display and analysis of macromolecular structures, *Journal of Molecular Graphics* 14, 51-55.
31. The PyMOL Molecular Graphics System, Version 1.7.4 Schrödinger, LLC.
32. Laskowski, R. A., MacArthur, M. W., Moss, D. S., and Thornton, J. M. (1993) PROCHECK: a program to check the stereochemical quality of protein structures, *Journal of applied crystallography* 26, 283-291.
33. Williamson, M. P. (2013) Using chemical shift perturbation to characterise ligand binding, *Progress in Nuclear Magnetic Resonance Spectroscopy* 73, 1-16.
34. Doyle, J. J., and Doyle, J. L. (1987) A rapid DNA isolation procedure for small quantities of fresh leaf tissue, *Phytochemical Bulletin* 19, 11-15.
35. Petersen, T. N., Brunak, S., von Heijne, G., and Nielsen, H. (2011) SignalP 4.0: discriminating signal peptides from transmembrane regions, *Nature methods* 8, 785-786.
36. Hall, T. A. (1999) BioEdit: a user-friendly biological sequence alignment editor and analysis program for Windows 95/98/NT, *Nucleic Acids Symposium Series* 41, 95-98.
37. Lehrer, R. I., Rosenman, M., Harwig, S. S. S. L., Jackson, R., and Eisenhauer, P. (1991) Ultrasensitive Assays for Endogenous Antimicrobial Polypeptides, *J Immunol Methods* 137, 167-173.
38. Miller, X. H. a. W. (1991) A Time-Efficient, Linear-Space Local Similarity Algorithm *Advances in Applied Mathematics* 12 337-357.
39. Feeney, J., Batchelor, J. G., Albrand, J. P., and Roberts, G. C. K. (1979) Effects of Intermediate Exchange Processes on the Estimation of Equilibrium-Constants by Nmr, *J Magn Reson* 33, 519-529.
40. Lian, L. Y. (1993) Dynamic and exchange processes in macromolecules studied by NMR spectroscopy., *Methods in molecular biology (Clifton, N.J.)* 17, 169-189.
41. Klaus K. Nielsen*, j. E. N., Susan M. Madrid, and jorn D. Mikkelsen. (1997) Characterization of a New Antifungal Chitin-Binding Peptide from Sugar Beet Leaves, *Plant Physiol*, 83-91.
42. Jennings, C., West, J., Waite, C., Craik, D., and Anderson, M. (2001) Biosynthesis and insecticidal properties of plant cyclotides: The cyclic knotted proteins from *Oldenlandia affinis*, *P Natl Acad Sci USA* 98, 10614-10619.
43. Nguyen, G. K. T., Zhang, S., Wang, W., Wong, C. T. T., Nguyen, N. T. K., and Tam, J. P. (2011) Discovery of a Linear Cyclotide from the Bracelet Subfamily and Its Disulfide Mapping by Top-down Mass Spectrometry, *J Biol Chem* 286, 44833-44844.

44. Nguyen, P. Q. T., Luu, T. T., Bai, Y., Nguyen, G. K. T., Pervushin, K., and Tam, J. P. (2015) Allotides: Proline-Rich Cystine Knot α -Amylase Inhibitors from *Allamanda cathartica*, *Journal of Natural Products* 78, 695-704.
45. Mergaert, P., Nikovics, K., Kelemen, Z., Maunoury, N., Vaubert, D., Kondorosi, A., and Kondorosi, E. (2003) A novel family in *Medicago truncatula* consisting of more than 300 nodule-specific genes coding for small, secreted polypeptides with conserved cysteine motifs, *Plant Physiol* 132, 161-173.
46. De Bolle, M. F. C., David, K. M. M., Rees, S. B., Vanderleyden, J., Cammue, B. P. a., and Broekaert, W. F. (1993) <Cloning and characterization of a cDNA encoding an antimicrobial chitin-binding protein from amaranth, *Amaranthus caudatus*.pdf>, *Plant Mol Biol* 22, 1187-1190.
47. Andreev, Y. A., Korostyleva, T. V., Slavokhotova, A. A., Rogozhin, E. A., Utkina, L. L., Vassilevski, A. A., Grishin, E. V., Egorov, T. A., and Odintsova, T. I. (2012) Genes encoding hevein-like defense peptides in wheat: distribution, evolution, and role in stress response, *Biochimie* 94, 1009-1016.
48. Asensio, J. L., Canada, F. J., Bruix, M., Rodriguezromero, A., and Jimenezbarbero, J. (1995) The Interaction of Hevein with N-Acetylglucosamine-Containing Oligosaccharides - Solution Structure of Hevein Complexed to Chitobiose, *European Journal of Biochemistry* 230, 621-633.
49. Juan Felix Espinosa, J. L. A., Jose Luis Garcia, Jose Laynez, Marta Bruix, Christine Wright,, and Hans-Christian Siebert, H.-J. G., Francisco Javier Canada and Jesus Jimenez-Barbero. (2000) <NMR investigations of protein-carbohydrate interactions binding studies and refined three-dimensional solution structure of the complex between the B domain of wheat germ agglutinin and N,N',N''-triacylchitotriose.pdf>, *Eur. J. Biochem*, 3965-3978.
50. Verheyden, P., Pletinckx, J., Maes, D., Pepermans, H. A. M., and Wyns, L. (1995) <1H NMR study of the interaction of triacetyl chitotriose with Ac-AMP2, a sugar binding antimicrobial protein isolated from *A.caudatus*.pdf>, *FEBS Lett* 370, 245-249.
51. Juan L Asensio¹, F. J. C., Hans-Christian Siebert², José Laynez³, Ana Poveda⁴, P. M. N., UM Soedjanaamadja⁶, Hans-Joachim Gabius², and Jiménez-Barbero¹, a. J. (2000) <Structural basis for chitin recognition by defense proteins: GlcNAc residues are bound in a multivalent fashion by extended binding sites in hevein domains .pdf>, *Chemistry & Biology*, 529-543.